

## Energy dissipation above plane terraces of a model crystal in non-contact atomic force microscopy

This article has been downloaded from IOPscience. Please scroll down to see the full text article.

2002 J. Phys.: Condens. Matter 14 4329

(<http://iopscience.iop.org/0953-8984/14/17/306>)

[View the table of contents for this issue](#), or go to the [journal homepage](#) for more

Download details:

IP Address: 171.66.16.104

The article was downloaded on 18/05/2010 at 06:33

Please note that [terms and conditions apply](#).

# Energy dissipation above plane terraces of a model crystal in non-contact atomic force microscopy

L N Kantorovich

Physics and Astronomy, University College London, Gower Street, London, WC1E 6BT, UK

Received 18 October 2001, in final form 8 March 2002

Published 18 April 2002

Online at [stacks.iop.org/JPhysCM/14/4329](http://stacks.iop.org/JPhysCM/14/4329)

## Abstract

We re-examine the calculation of the dissipation energy in the non-contact atomic force microscope for a model flat surface within the stochastic friction force (the ‘Brownian motion’) mechanism. All important aspects of the problem are taken into account. In particular, we have considered for the first time: (i) the effect of the tip on the surface atom vibrations including the possibility of inducing local vibrational modes and (ii) the second term in the expansion of the fluctuating tip–surface force in atomic displacements. We found that generally, if the tip does not come very close to the surface, the first effect noticeably reduces the dissipation energy, while the second-order correction is very small, at least for the model planar surface considered. However, if during its oscillations the tip comes closer than a certain critical distance to the surface, a local vibrational mode is induced which may considerably increase the dissipation energy depending on its lifetime, i.e. the degree of anharmonicity in the system coupling the local mode (LM) with the rest of the phonons. For certain systems which provide long-living LMs, this effect may serve as a microscopic mechanism of energy dissipation. We also demonstrate that the dissipation power increases with the tip oscillation amplitude.

## 1. Introduction

An important step toward strengthening the success of large-amplitude non-contact atomic force microscopy (NC-AFM) [1–10] would be widening its possible range of applications. The conservative component of the tip–surface interaction has been the main focus of most of the theoretical and experimental work. These studies have been extremely successful, as true atomic resolution has been achieved for a number of crystal surfaces of non-conducting materials [11–13] and the basic physics seems to be clear [14–20]. However, there is also another, namely *stochastic*, component of the interaction which has received attention only recently [11, 14, 20–23]. Although atomic resolution has also been obtained in some cases [11, 12, 24], the nature of the dissipation processes in the NC-AFM system is far from being well understood.

Three models have been suggested so far to explain energy dissipation in the NC-AFM. The main idea of the *adhesion hysteresis* mechanism [25] (borrowed from tapping mode microscopy [26]) is based on atomic processes caused by the approaching and then retracting tip during the close approach: the tip distorts potential energy surfaces (e.g. reduces barriers) for atoms in its proximity in such a way that it may be more feasible for them to jump from one potential energy minimum to the other. The energy gain is then transferred to the lattice phonons, essentially leading to energy dissipation of the order of typical energies of atomic processes (0.1–2 eV per oscillation cycle), which is in within the range of values measured in experiments [11, 12, 15, 23]. Note that so far this mechanism has been considered only statically; its non-equilibrium nature [27] has not yet been sufficiently explored.

Two other models exploit the *stochastic* aspect of the tip–surface interaction more directly. In [28] it is suggested that a macroscopic current associated with the tip movement during oscillations results in an energy dissipation due to dynamic image interaction with the surface. However, it is argued in [29] that the proposed mechanism should give energies which are much smaller than experimentally observed.

In this paper we shall consider another mechanism: the so-called *stochastic friction force mechanism* [27, 30–32]. According to this, the stochastic component in the tip–surface force is caused by vibrations of atoms in a microscopic region of the junction. This includes atoms of the surface which are in the tip proximity and also atoms at the tip end (the nano-tip). In a sense the tip performs as an oscillating Brownian particle moving on a much slower timescale than vibrating atoms. The latter never establish complete thermodynamic equilibrium because of the constantly moving tip. As a result of this *non-equilibrium* process, a friction force  $F_{frict}(Q, \dot{Q}) = -\xi(Q)\dot{Q}$ , proportional to the tip velocity  $\dot{Q}$ , appears which is responsible for the energy dissipation. Here  $Q$  is the vertical position of the tip with respect to the surface and

$$\xi(Q) = \beta\gamma(Q) = \beta \lim_{z \rightarrow +i0} \gamma(Q, z) = \beta \lim_{z \rightarrow +i0} \int_0^\infty e^{izt} \gamma(Q, t) dt \quad (1)$$

is the corresponding friction coefficient defined [32] via the Laplace transform of the fluctuating tip–surface force autocorrelation function

$$\gamma(Q, t) = \langle \Delta X(Qq) e^{it\hat{L}} \Delta X(Qq) \rangle_{eq} = \langle \Delta X(Qq(0)) \Delta X(Qq(t)) \rangle_{eq}. \quad (2)$$

Here  $\beta = 1/k_B T$  is the inverse temperature and  $t$  is time. The exponential factor in equation (1) has been introduced to ensure convergence of the integral at the upper limit. The angle brackets indicate the equilibrium statistical average for the tip fixed at  $Q$ ; i.e. the statistical average is calculated using the *equilibrium* distribution function  $f_0^{(N)}(pq)$  associated with the fast subsystem (atomic vibrations), the coordinates and momenta of which are denoted by the column matrices  $q$  and  $p$ . In addition,  $q(t)$  corresponds to the classical evolution of the atomic coordinates with time. The fluctuation of the force  $\Delta X(Qq)$  is defined as  $\Delta X(Qq) = X(Qq) - \langle X(Qq) \rangle_{eq}$ , where  $X(Qq) = -\partial\Phi_{Qq}/\partial Q$  is the instantaneous tip–surface force calculated for the current positions  $q$  of all atoms,  $\Phi_{Qq}$  is the interaction energy of the tip and the surface. Since we are interested in the fluctuation of the tip–surface force, which appears as a *difference* between the instantaneous and the average forces, it is clear that only part of the total interaction which depends explicitly on the atomic positions is relevant here. Therefore, for the sake of simplicity in what follows we shall call that part of the total force the tip–surface force. It includes direct interactions between atoms of the nano-tip and the surface. Other interactions such as the van der Waals interaction and that arising due to applied bias (the capacitance force) serve as a conservative part of the force and are irrelevant to the problem studied here.

The first estimate of the dissipation energy associated with this mechanism was made in [30] using a very simple model in which the surface has been modelled by a single atom.

The calculated dissipation energies turned out also to be much too small in comparison with those observed experimentally. In [32] a better model was suggested: although the tip has been allowed to interact with only one surface atom directly underneath it (called the first atom), this atom interacted with all surface atoms which all were allowed to relax. Significantly larger dissipation energies have been obtained, although still several orders of magnitude smaller than in the experiment.

It seems that it follows from these first calculations that the stochastic friction force mechanism cannot explain observed energy losses in the NC-AFM. However, before we reach such a conclusion, we have to consider carefully all the approximations made in the treatment of [32]. In particular, while calculating the friction, the phonon Green function of the tip-free surface has been used in [32], i.e. the effect of the tip on the vibrations of surface atoms has not been accounted for. In addition, as in [30], only the first term in the expansion of the tip-surface force in atomic displacements has been included. Therefore, the purpose of the present paper is to extend our previous treatment of the model surface considered in [32] and include these two additional effects in order to check the validity of the theory.

Therefore, in the next section a general expression for the friction via the surface Green function is obtained up to the second term in the expansion of the force autocorrelation function (2) with respect to atomic displacements. In section 3 our model surface system will be introduced and the final expression for the friction coefficient will be developed including the effect of the local modes (LMs) induced by the tip. Results of the calculations will be presented in section 4 and the conclusions will be drawn in section 5.

## 2. General expression for the friction coefficient

To calculate the friction coefficient given by equations (1) and (2), we use the same method as in our previous work [32]. The surface and the nano-tip are considered as a set of interacting atoms: a finite cluster is used to model the nano-tip while an infinite number of atoms is used to model the surface. Therefore, we explicitly use a discrete model for the surface. Then, we expand the fluctuation of the tip-surface force  $X(Qq)$  in a power series with respect to atomic displacements  $u_{i\alpha} = q_{i\alpha} - q_{i\alpha}^0$ :

$$\Delta X(Qq) = \sum_{i\alpha} X_{i\alpha}(Qq_0)u_{i\alpha} + \frac{1}{2} \sum_{i'\alpha\alpha'} X_{i\alpha,i'\alpha'}(Qq_0)\{u_{i\alpha}u_{i'\alpha'} - \langle u_{i\alpha}u_{i'\alpha'} \rangle_{eq}\} + \dots \quad (3)$$

where  $i, i'$  designate atoms of the surface and those of the nano-tip, and the Greek indices are used for Cartesian components of vectors and tensors. The column-matrix  $q_0 = ||q_{i\alpha}||$  represents equilibrium positions of the atoms when the tip is fixed at  $Q$ . Note that  $q_0$  depends explicitly on  $Q$ , i.e.  $q_0 = q_0(Q)$ . It is obtained by minimizing the total potential energy of the whole system. The vector  $X_1 = ||X_{i\alpha}(Qq_0)||$  and the matrix  $X_2 = ||X_{i\alpha,i'\alpha'}(Qq_0)||$  are given as derivatives of the tip-surface interaction energy and can be calculated for the given interaction model.

Inserting expansion (3) into equation (2), we will arrive at a sum of terms containing various displacement-displacement correlation functions. The first non-vanishing term, the displacement-displacement correlation function, has been considered previously [32]. Similarly, one can work out higher-order contributions. Let  $D$  be the dynamical matrix of the combined system (surface + nano-tip), whose eigenvalues and eigenvectors are  $\omega_\lambda$  and  $e_\lambda = ||e_{i\alpha}(\lambda)||$ . Then, the next non-vanishing term in  $\gamma(Q, t)$  of equation (2) will be of the fourth order:

$$\gamma_2(Q, t) = \frac{1}{4} \sum_{\lambda_1\lambda_2} \sum_{\lambda_3\lambda_4} \Lambda_{\lambda_1\lambda_2} K_{\lambda_1\lambda_2;\lambda_3\lambda_4} \Lambda_{\lambda_3\lambda_4} \quad (4)$$

where

$$K_{\lambda_1\lambda_2;\lambda_3\lambda_4} = \langle (\zeta_{\lambda_1}\zeta_{\lambda_2} - \langle \zeta_{\lambda_1}\zeta_{\lambda_2} \rangle_{eq})(\zeta_{\lambda_3}(t)\zeta_{\lambda_4}(t) - \langle \zeta_{\lambda_3}\zeta_{\lambda_4} \rangle_{eq}) \rangle_{eq} \quad (5)$$

is the corresponding correlation function in this case and we introduced a quantity  $\Lambda_{\lambda_1\lambda_2} = \mathbf{e}_{\lambda_1}^\dagger \mathbf{D}_2 \mathbf{e}_{\lambda_2}$ , where  $\mathbf{D}_2 = \mathbf{M}^{-1/2} \mathbf{X}_2 \mathbf{M}^{-1/2}$ . Necessary classical statistical averages can be easily calculated as  $\langle \zeta_\lambda \zeta_{\lambda'} \rangle_{eq} = \delta_{\lambda\lambda'} / \beta \omega_\lambda^2$ ,  $\langle \eta_\lambda \eta_{\lambda'} \rangle_{eq} = \delta_{\lambda\lambda'} / \beta$  and

$$K_{\lambda_1\lambda_2;\lambda_3\lambda_4} = \frac{1}{\beta^2} (\delta_{\lambda_1\lambda_3} \delta_{\lambda_2\lambda_4} + \delta_{\lambda_1\lambda_4} \delta_{\lambda_2\lambda_3}) \frac{\cos(\omega_{\lambda_1} t)}{\omega_{\lambda_1}^2} \frac{\cos(\omega_{\lambda_2} t)}{\omega_{\lambda_2}^2}. \quad (6)$$

Here  $(\zeta_\lambda)$  and  $(\eta_\lambda = \dot{\zeta}_\lambda)$  are conjugate normal coordinates and momenta. Inserting equation (6) in (4), introducing a matrix function [32]

$$\Gamma(t) = \sum_{\lambda} \frac{\mathbf{e}_\lambda \mathbf{e}_\lambda^\dagger}{\omega_\lambda^2} \cos(\omega_\lambda t) \quad (7)$$

and using the fact that  $\Lambda_{\lambda_1\lambda_2} = \Lambda_{\lambda_2\lambda_1}$ , we obtain

$$\gamma_2(Q, t) = \frac{1}{2\beta^2} \text{Tr}(\Gamma(t) \mathbf{D}_2 \Gamma(t) \mathbf{D}_2). \quad (8)$$

The corresponding second-order contribution to the friction coefficient of equation (1) is then easily calculated as

$$\xi_2(Q) = \lim_{z \rightarrow +i0} \beta \gamma_2(Q, z) = \frac{\pi}{\beta} \int_0^\infty \text{Tr}[(\tilde{\Gamma}(\omega) \mathbf{D}_2)^2] d\omega \quad (9)$$

where

$$\tilde{\Gamma}(\omega) = \frac{1}{|\omega|} \sum_{\lambda} \mathbf{e}_\lambda \mathbf{e}_\lambda^\dagger \delta(\omega^2 - \omega_\lambda^2) \equiv -\frac{1}{\pi |\omega|} \text{Im } \mathbf{G}(\omega^2 + i0) \quad (10)$$

is the Fourier transform of  $\Gamma(t)$  and  $\mathbf{G}(z) = (z\mathbf{1} - \mathbf{D})^{-1}$  is the phonon Green function. Note that while deriving this expression we have made use of the fact that  $\tilde{\Gamma}(\omega)$  is an even function of  $\omega$ ; see equation (10). Note that since  $\tilde{\Gamma}(\omega)$  is proportional to the imaginary part of the Green function, the second part of equation (10), it is actually non-zero only up to some maximum phonon frequency  $\omega_{max}$ , so the integration above is in fact finite. At the bottom of the integration interval the integral also converges since, as can easily be shown,  $\tilde{\Gamma}(\omega)$  has a well defined  $\omega \rightarrow 0$  limit.

Several points are worth mentioning here. Firstly, contrary to the case of the first contribution to the friction [32], *all* phonons contribute to the integral above. In particular, if there are *local vibrational modes* (LMs) either due to a defect (e.g. adsorbed species) or directly induced by the tip, then these will also contribute to  $\xi_2(Q)$ . Note that the LMs do not contribute to the first component,  $\xi_1(Q)$ , of the friction. Secondly, since the interaction between the tip and the surface is of a certain finite radius,  $\mathbf{D}_2$  is actually a *finite* square matrix, so the matrix multiplications in equation (9) can be performed in practice for every  $Q$ . Thirdly, as in the case of the first-order contribution, the information about the vibrations in the combined system is all expressed via the Green function according to equation (10). It can easily be seen that this is the case for any other higher-order term which we, however, do not consider in this paper. Note that the Green function should depend on the tip position  $Q$  as well. Recall that this dependence has not been taken into account in our previous work [32]. Finally, unlike the first contribution, the second one is proportional to the absolute temperature, i.e. it linearly increases with  $T$  (recall that our present consideration is entirely classical).

Thus, summarizing, if we know the interaction between the atoms of the combined system (surface + nano-tip), then for every tip position  $Q$  we can calculate their equilibrium positions

$q_0$ , the corresponding dynamical matrix  $\mathbf{D}$  at  $q_0$  and, therefore, the Green function  $\mathbf{G}(z)$ . In addition, by expanding the interaction energy  $\Phi_{Qq}$  between atoms of the surface and those of the nano-tip in atomic displacements and differentiating it with respect to  $Q$ , we can obtain the vector  $\mathbf{X}_1$  and the matrix  $\mathbf{X}_2$  of the expansion (3). Using this information, one can calculate (at least, in principle) various contributions to the friction coefficient  $\xi(Q) = \xi_1(Q) + \xi_2(Q) + \dots$ , the first two of which have been discussed above. Note that further terms in this expansion can be similarly developed as well, but the expressions become more cumbersome. Once the friction coefficient is known, the average dissipation power  $\bar{P}$  can also be calculated as discussed e.g. in [23, 30, 32]. In the next section a simple model for a rigid tip interacting with a planar surface will be considered for which the formalism developed will be illustrated.

### 3. Calculation for a model plane surface

#### 3.1. Model

To calculate the dissipation energy, essentially the same model as in our previous work will be used [32]. The tip is considered as rigid, i.e. the nano-tip is simulated by just one atom at the tip end which is not allowed to relax. The surface consists of identical atoms of mass  $m$  arranged into a simple cubic lattice. The interaction of the tip atom with the surface is given by a sum of pairwise interactions with all surface atoms  $\Phi_{Qq} \equiv \sum_i \phi(Q - q_i)$ . Here the coordinates  $q_i = ||q_{i\alpha}||$  of surface atoms correspond to their displacements from the perfect lattice positions. The strongest (and dominant) interaction is with the closest surface atom (called the *first atom* [30]) which is lying directly under the tip. Therefore, we shall adopt here the simplest approximation [30, 32] in which the tip–surface interaction is modelled by that between the tip and the first surface atom only:  $\Phi_{Qq} \equiv \phi(Q - q_{1z})$ . This interaction depends on the distance  $Q - q_{1z}$  between the tip atom, whose vertical position with respect to the geometrical surface plane is  $Q$ , and the vertical coordinate of the first atom  $q_{1z}$ . Note that this approximation is not crucial and can be easily extended for a proper numerical calculation. However, qualitative insight into the problem can already be gained within this approximation, which allows analytical calculation of the phonon Green function. It is expected that the friction coefficient calculated within this model will be up to an order of magnitude smaller than that calculated using the full treatment in which interactions with all surface atoms are taken into account.

Following the method developed in [32], we assume that  $|q_{1z}| \ll Q$  and expand  $\Phi_{Qq}$  in a power series with respect to  $q_{1z}$ . Then, the force constant matrix will be given by

$$\Theta = ||\Theta_{i\alpha, i'\alpha'}|| = \Theta_0 + ||\delta_{i1} \delta_{\alpha z} \delta_{i'1} \delta_{\alpha'z} \phi''(Q)||. \quad (11)$$

Here,  $\Theta_0 = ||\Theta_{i\alpha, i'\alpha'}^0||$  is the corresponding force constant matrix of the perfect surface (i.e. without the tip). As one can see, the interaction with the tip results in a local perturbation to the matrix  $\Theta_0$ . Note that within this model the only non-zero elements of the vector  $\mathbf{X}_1$  and matrix  $\mathbf{X}_2$  are  $X_{1z} = \phi''(Q) - \phi'''(Q)q_{1z}^0$  and  $X_{1z,1z} = -\phi'''(Q)$ . This is a consequence of the fact that the tip interacts only with the coordinate  $q_{1z}$  of the first atom.

#### 3.2. The Green function of the combined tip–surface system

As discussed in section 2, the Green function is an essential ingredient of the two contributions to the friction coefficient. To calculate it we notice that the local perturbation to the force constant matrix  $\Theta_0$  of the perfect surface discussed above results in the only non-zero element of the perturbation  $W_{1z,1z} = -\phi''(Q)/m$  to the dynamical matrix  $\mathbf{D}_0$  of the perfect surface.

Since only the  $1z, 1z$  element of the Green function will be needed in our model (see below), we easily obtain using simple and standard manipulations:

$$G_{1z,1z}(z) = \frac{G_{1z,1z}^0(z)}{1 - (\phi''(Q)/m)G_{1z,1z}^0(z)} \quad (12)$$

where  $G_0(z) = (z\mathbf{1} - \mathbf{D}_0)^{-1}$  is the Green function of the perfect surface.

To calculate  $G_{1z,1z}^0(z)$ , we shall use the same trick as in our previous work [32] and assume that  $G_0$  can be modelled by the bulk Green function. Then, its diagonal elements are all the same and can be linked to the phonon density of states (DOS)  $\aleph(\omega) = \sum_\lambda \delta(\omega - \omega_\lambda)$  of the perfect crystal as follows:

$$G_{1z,1z}^0(z) = \frac{1}{3N} \text{Tr } G(z) = \frac{1}{3N} \int_0^\infty \frac{\aleph(\omega) d\omega}{z - \omega^2} \equiv R_0(\omega) + iI_0(\omega) \quad (13)$$

where the real and imaginary parts (in the limit  $z \rightarrow \omega^2 + i0$ ) are given by:  $R_0(\omega) = -\lambda m \vartheta(x)$  and  $I_0(\omega) = -(\pi/2)m\lambda|x|$ . Here the Debye model for the phonon DOS has been used. In addition,  $\lambda = (3/mc^2)(v_c/6\pi^2)^{2/3}$  is a constant,  $c$  an effective sound velocity in the crystal,  $v_c$  the bulk unit cell volume;  $x = \omega/\omega_D$  is a relative frequency,  $\omega_D = c(6\pi^2/v_c)^{1/3}$  being the Debye frequency, and the function  $\vartheta(x) = 1 + (x/2) \ln |(x-1)/(x+1)|$ . Note that  $I_0(\omega) \neq 0$  only when  $|x| \leq 1$  (i.e. for  $|\omega| \leq \omega_D$ ).

Calculating the imaginary part of the Green function (12), we can finally calculate  $\Gamma_{1z,1z}(\omega)$  by virtue of equation (10). For  $|x| \leq 1$  we obtain

$$\Gamma_{1z,1z}(\omega) = \frac{v_c}{4\pi^2 c^3} \left\{ [1 + \lambda\phi''(Q)\vartheta(x)]^2 + \left[ \frac{\pi}{2} \lambda\phi''(Q)x \right]^2 \right\}^{-1} \quad (14)$$

where, as before,  $x = \omega/\omega_D$ . One can see that  $\Gamma_{1z,1z}(\omega)$  is a well defined function at  $\omega = 0$ .

### 3.3. Local modes

It follows from the structure of the system Green function (12) that in certain circumstances LMs can exist. Indeed, beyond the spectrum of the free surface, i.e. when  $\omega > \omega_D$ , we have  $\text{Im } G_{1z,1z}^0(\omega^2 + i0) = 0$ . Therefore, if the real part of the denominator is equal to zero for some  $\omega = \omega_{LM} > \omega_D$ , i.e. if

$$g(x) \equiv 1 + \lambda\phi''(Q)\vartheta(x) = 0 \quad (15)$$

for some  $x \equiv x_{LM} = \omega_{LM}/\omega_D > 1$ , then the Green function would have a pole which should contribute to the friction as well. It is easily verified that in our model only a single solution  $x_{LM} > 1$  is possible provided that  $\phi''(Q) > 0$ . As will be seen later on, this condition imposes certain limitations on the  $Q$ -values for which the LMs can exist.

To calculate the contribution of the LMs to the friction  $\xi_2(Q)$  (this will be done in the next subsection), we will need an expression for the imaginary part of the Green function (12) at  $z = \omega_{LM}^2 + i\epsilon$  with a small but finite  $\epsilon$ :

$$\text{Im } G_{1z,1z}(\omega^2 + i\epsilon) = -\frac{6\pi x_{LM}}{(\lambda\phi''(Q))^2 \vartheta'(x_{LM})} \Delta_\epsilon((x - x_{LM})g_1) \quad (16)$$

where  $g_1 = g'(x_{LM}) = 2\omega_D^2 x_{LM} > 0$  and  $\Delta_\epsilon(x) = (1/\pi)\epsilon/(\epsilon^2 + x^2)$ . The latter function tends to the delta function in the  $\epsilon \rightarrow +0$  limit. Thus, as one would expect, the imaginary part of the Green function at the LM is proportional to the delta function  $\delta(\omega - \omega_{LM})$  and so is the function  $\Gamma_{1z,1z}(\omega)$  according to equation (10).

### 3.4. First- and second-order contributions to the friction

As has been shown in [32], the first-order contribution to the friction  $\xi_1(Q)$  in our model is expressed via  $\Gamma_{1z,1z}(0)$ . However, it has been calculated in [32] without taking into account the extra term in  $\Theta$  of equation (11), i.e. by assuming that the tip does not affect the vibrations of the surface atoms. The same approximation has been effectively used in [30]. This approximation can be easily dispensed with if we use equation (14) for  $\Gamma_{1z,1z}(\omega)$ . Setting  $x = 0$  there, we obtain

$$\Gamma_{1z,1z}(0) = \frac{v_c}{4\pi^2 c^3} \frac{1}{(1 + \lambda\phi''(Q))^2}. \quad (17)$$

The difference from our previous result of [32] is in an additional second factor which is  $Q$ -dependent.

The second contribution to the friction coefficient is calculated in accordance with equation (9). As the integration there is performed over the whole frequency range, there may be two contributions. As mentioned above, the only non-zero element of the matrix  $X_2$  is  $X_{1z,1z} = -\phi'''(Q)$ , so the first contribution, due to the continuum  $0 \leq \omega \leq \omega_D$  in the spectrum of the tip-free surface, is

$$\xi_2^{(1)}(Q) = \frac{\pi\lambda^2}{4\beta\omega_D} [\phi'''(Q)]^2 \int_0^1 \left\{ [1 + \lambda\phi''(Q)\vartheta(x)]^2 + \left[ \frac{\pi}{2} \lambda\phi''(Q)x \right]^2 \right\}^{-2} dx \quad (18)$$

where the explicit expression (14) for  $\Gamma_{1z,1z}(\omega)$  has been used. In our calculations the integration here has been performed numerically.

If LMs exist, there will also be an additional contribution to  $\xi_2(Q)$ . If we use, however, our result from section 3.3, we would obtain an integral of the square of the delta function which is *infinite*. This seemingly paradoxical result is the consequence of the harmonic approximation. Indeed, the LM, being a vibrational mode separated from the continuum of other phonon modes, corresponds to a single harmonic oscillator. However, in this case the corresponding time autocorrelation functions do not decay with time and, therefore, their Laplace transform is infinite. Recall, for example, that the  $t^{-1}$ -decay of the displacement autocorrelation function [32] follows from the integration over frequencies within the continuum of the tip-free system.

Therefore, it is clear, that in order to take account of the LMs one has to go *beyond* the harmonic approximation. As we are interested in this paper mostly in drawing a qualitative picture of the dissipation phenomenon in the NC-AFM, we have used a simple model corresponding to the so-called *quasiparticle* approximation [33]. In this case the Green function is formally similar to that of the harmonic model, but the frequencies  $\omega_\lambda$  acquire a complex part  $i/\tau_\lambda$ , where  $\tau_\lambda$  is the finite lifetime of the harmonic phonon  $\lambda$ . In this approximation one gets  $\Delta_\epsilon(\omega^2 - \omega_\lambda^2)$  instead of  $\delta(\omega^2 - \omega_\lambda^2)$  in the expression for the imaginary part of the Green function with  $\epsilon = 2\omega_\lambda/\tau_\lambda$  which is different for every phonon mode  $\lambda$ .

Thus, in order to calculate the contribution of the LM to the friction coefficient  $\xi_2(Q)$ , we have to calculate the contribution to the integral in equation (9) due to frequencies  $\omega > \omega_D$  and we shall use the quasiparticle model for that. In practice, we use equation (16) for the imaginary part of the Green function in which we set  $\epsilon = 2\omega_{LM}/\tau_{LM} = 2x_{LM}\omega_D^2/\tau$ . Here the lifetime  $\tau_{LM}$  is measured in terms of the inverse of the Debye frequency:  $\tau_{LM} = \tau/\omega_D$ . The corresponding integral over frequencies  $\omega \geq \omega_D$  is then calculated approximately by extending the lower limit to  $-\infty$ , so the final contribution to the friction reads

$$\xi_2^{(2)}(Q) = \frac{\lambda^2\tau}{2\beta\omega_D x_{LM}} \left( \frac{\phi'''(Q)}{(\lambda\phi''(Q))^2\vartheta'(x_{LM})} \right)^2. \quad (19)$$

We see that it is proportional to the parameter  $\tau$  and becomes infinite in the harmonic approximation when  $\tau = \infty$ . By assuming finite values of  $\tau$ , we shall take approximate account of the phonon coupling, i.e. of the anharmonicity in the surface vibrations.

Note that if we used the Green function of the tip-free surface while calculating this contribution, i.e. if we neglected the effect of the tip on vibrations of surface atoms, then we would obtain the result in which the integral in equation (18) is set to one and there will be no contribution due to the LMs. As will become clear from the next section, this approximation has a dramatic effect on  $\xi_2(Q)$ .

#### 4. Results

As in the previous study [32], the following values for the constants have been used:  $m = 33.2 \times 10^{-27}$  kg,  $v_c = 10^{-29}$  m<sup>3</sup> and  $c = 5 \times 10^3$  m s<sup>-1</sup>, so  $\lambda = 0.1769$  Å<sup>2</sup> eV<sup>-1</sup>. Depending on the chemical nature of the tip atom and the first surface atom, various types of tip–surface interaction can be envisaged. Note that we are interested only in the microscopic (i.e. ‘chemical’) interaction between tip and surface, as it is the only part of the overall tip–surface interaction which contributes to the friction [32]. Conservative interactions such as the van der Waals and electrostatic (capacitance) contributions to the overall tip–surface force do not lead to energy loss and, therefore, are not considered here. To give some qualitative account of the effect on the friction of different types of interaction, two qualitatively different models are considered in this paper: short-range attractive and long-range repulsive interactions  $\phi(Q)$ . This choice is perfectly valid since during its large-amplitude oscillations the tip samples a wide range of distances and the system is in general far from equilibrium. As in [32], attractive interaction has been modelled using the Lennard-Jones (LJ) potential  $\phi(Q) = 4\epsilon[(\sigma/Q)^{12} - (\sigma/Q)^6]$  with  $\epsilon = 2.315$  eV and  $\sigma = 2.35$  Å, while the repulsive potential has been simulated by a simple Coulomb interaction  $\phi(Q) = e^2/Q$ ,  $e$  being the elementary charge. One should bear in mind, however, that our model is greatly oversimplified and probably does not work at distances around 2 Å and below, so the results corresponding to small tip–surface distances should be considered with care.

First of all, we discuss the calculation of the friction coefficient. The first-order contribution is shown in figure 1. Results of two sets of calculations are shown. Dotted curves demonstrate the friction coefficients calculated using the Green function of the perfect surface, i.e. without the influence of the tip on the vibrations of surface atoms (model I). This corresponds to dropping the second factor in equation (17) for  $\Gamma_{1z,1z}(0)$ . Solid curves show the full calculation in which the effect of the tip on the surface vibrations has been taken into account (model II). It is seen that this effect drastically reduces the calculated friction coefficient; this is especially noticeable for the LJ potential. In addition, the friction is cut at small tip–surface distances in the LJ case: if the effect of the tip on surface vibrations is neglected, the friction sharply and indefinitely grows with approach; however, if this effect is included, the friction drops to zero at around 2.5 Å. Thus, in the case of the attractive LJ interaction the friction coefficient  $\xi_1(Q)$  appears to be essentially non-zero within a finite interval of the tip–surface distances, somewhere between 2.5 and 4 Å.

In calculating the second-order contribution to the friction, equations (18) and (19), we have to study first whether there is a LM in the first place. A simple calculation of  $\phi''(Q)$  as a function of  $Q$  gives us the necessary criteria. For the case of the attractive LJ potential,  $\phi''(Q) > 0$  only for  $Q$  smaller than some critical distance  $Q_{crit} = 2.925$  Å. At this distance the LM splits off from the top of the phonon band at  $\omega_D$  and then moves out toward higher frequencies as the tip approaches. This is seen in figure 2. The effect is very strong in the case of the attractive LJ interaction. Interestingly,  $\phi''(Q)$  remains positive for all  $Q$  in the repulsive

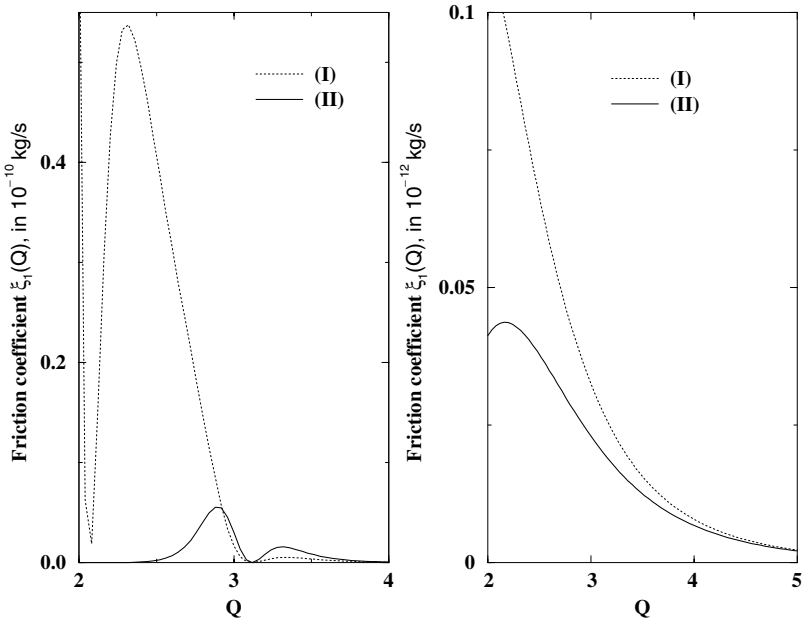


**Figure 1.** The first part of the friction coefficient,  $\xi_1(Q)$ , for the LJ (the left panel, in units of  $10^{-10} \text{ kg s}^{-1}$ ) and the Coulomb  $e^2/Q$  potentials (the right panel, in units of  $10^{-12} \text{ kg s}^{-1}$ ) as a function of the tip distance  $Q$  (in Å) to the surface. The dotted curves correspond to model I, the full lines to model II (see the text).

case considered here, so there is a LM at any  $Q$ . However, the position of the LM,  $x_{LM}$ , does not move very much with  $Q$ , staying just above 1 at all tip positions.

The calculated second-order contribution to the friction is shown in figure 3. Model I corresponds to the calculation in which the effect of the tip on the lattice vibrations is completely neglected. This means that, while calculating the contribution due to the phonon continuum  $\omega \in [0, \omega_D]$ , the integral in equation (18) for  $\xi_2^{(1)}(Q)$  is set to one and the LM contribution is also neglected. The solid curve corresponding to model II shows the full calculation of  $\xi_2^{(1)}(Q)$  in which the effect of the tip on the surface vibrations has been taken into account. The contribution of the LMs,  $\xi_2^{(2)}(Q)$ , calculated using  $\tau = 10$  is shown by a dash-dotted curve. In the case of the LJ potential this contribution switches on at  $Q_{crit}$  and then grows rapidly with the approach of the tip. In the case of the repulsive interaction the LM contribution is extremely small for all  $Q > 2 \text{ \AA}$  and becomes noticeable only at very close approach below 2 Å when our model probably does not work (not shown).

We see that the effect of the tip on the vibrations of surface atoms has a dramatic effect on the calculated friction coefficient: the first-order contribution,  $\xi_1(Q)$ , as well as the continuum contribution to the second-order friction coefficient,  $\xi_2^{(1)}(Q)$ , are noticeably reduced, especially in the LJ case. However, at small distances there is also a LM contribution which can substantially increase the friction and compensate for the drop. In the calculations shown in figure 3 the parameter  $\tau = 10$  (i.e.  $\tau_{LM} = 10/\omega_D$ ). For this value of  $\tau$  the overall second-order contribution is at least two orders of magnitude smaller than the first-order one. This demonstrates that the expansion series that we have been using in the calculation of the fluctuating force autocorrelation function is essentially converged for the plane surface considered here already in the first-order term. In addition, the friction is found to be much smaller for the repulsive interaction [32]. Finally, in the case of the attractive interaction each

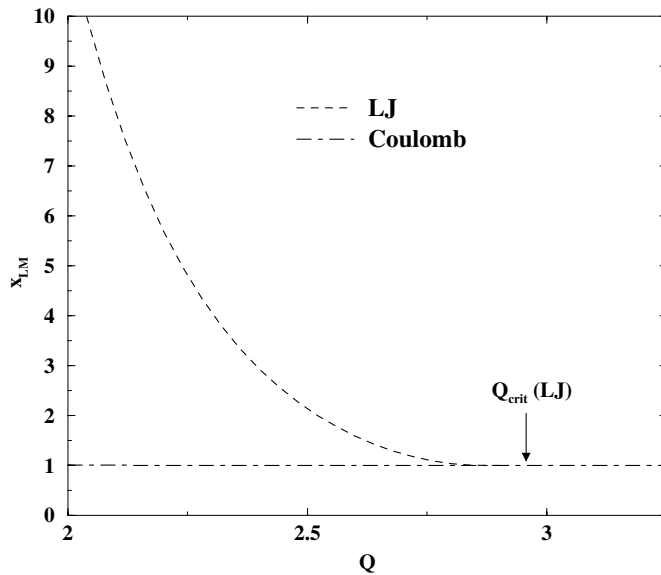


**Figure 2.** Solutions of equation (15),  $x_{LM} = \omega_{LM}/\omega_D$ , for different values of  $Q$  (in Å) for the LJ and repulsive Coulomb potentials  $\phi(Q)$ . The critical distance  $Q_{crit}$  in the case of the LJ potential is indicated by an arrow.

component of the friction coefficient has a characteristic two-peak structure which, as has been already discussed previously [32], is due to surface relaxation effects which depend on the position  $Q$  of the tip. The friction coefficient varies much more smoothly in the case of the repulsive interaction potential.

The calculation of the dissipation power has been performed in a standard way using numerical integration over the tip trajectory of the work done by the friction force [23, 30, 32]. Two oscillation amplitudes  $A_0$  have been considered: 36 Å (case A) and 100 Å (case B). In each case we used the oscillation frequency of  $1.58 \times 10^5$  Hz which is typical for the large-amplitude NC-AFM [11]. Also, in all our calculations the temperature  $T$  has been fixed at 300 K. Note that only the second-order term changes with temperature.

The results of our calculations for the attractive and repulsive interactions are shown in figures 4 and 5, respectively. In these calculations  $\tau = 10$ . Firstly, we notice that the features of the friction discussed above are reflected in the calculated dissipation power:

- (i) If in model I the power due to the first term in friction sharply grows with the approach to the surface, its increase is substantially reduced in model II and the power becomes generally smaller.
- (ii) The continuum contribution to the power due to the second part of the friction is also substantially reduced in model II, but this effect is overpowered by the corresponding contribution of the LMs at small distances.
- (iii) The power due to the second-order term is about two orders of magnitude smaller than that calculated using the first-order term. This means that at least for the plane surface considered here and the value of  $\tau = 10$  the first-order term is essentially sufficient. However, as will be shown below, the result is very sensitive to the unknown parameter  $\tau$ .
- (iv) The dependence of the power on the distance of closest approach is much smoother for the repulsive interaction in comparison with that of the attractive one.
- (v) Finally, we see that the power generally grows with the oscillation amplitude.

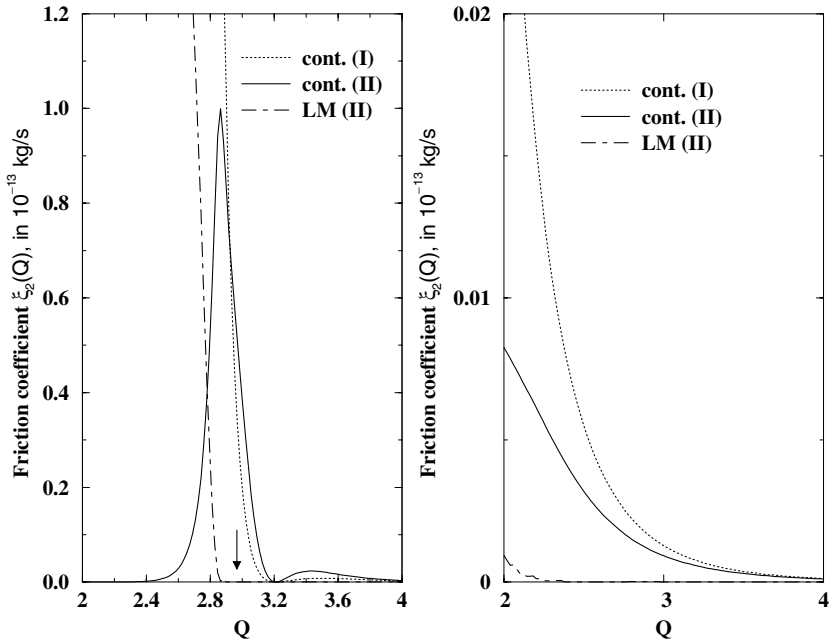


**Figure 3.** The second part of the friction coefficient,  $\xi_2(Q)$  (in units of  $10^{-13} \text{ kg s}^{-1}$ ), for the LJ (the left panel) and the Coulomb  $e^2/Q$  (the right panel) potentials as a function of the tip–surface distance  $Q$  (in Å). The contributions of the surface phonon continuum  $\omega \in [0, \omega_D]$  in models I and II (see the text) are shown by the dotted and solid curves, respectively (marked ‘cont.’), while the contributions of the LMs (for  $\tau = 10$ ) are shown by the dash-dotted curves. An arrow indicates the critical distance  $Q_{crit}$  for the LJ case.

It is seen from the results presented above that with the choice of  $\tau = 10$  the calculated dissipation power is much smaller than that observed in experiment. This formally agrees with the earlier estimates [30, 32]. However, the value of  $\tau$  is actually unknown. It characterizes the coupling between the LMs and other phonons: the smaller  $\tau$ , the larger the coupling and vice versa. Since the LM phonon lifetime is not easy to calculate or estimate, it is instructive at this stage to see how the dissipation effect changes with  $\tau$ . The dependence of the dissipation energy (per oscillation cycle) on  $\tau$  for the first-order and the second-order contributions is shown in figure 6 for the LJ potential. Note that the second-order contribution is almost entirely due to the LMs. It appears that the contribution of the LMs in the case of the repulsive Coulomb potential is much smaller than the first-order contribution,  $\xi_1(Q)$ , even for  $\tau = 500$ , and the final dissipation energies are very small. Therefore, we do not show the corresponding graph for this case. The situation is different in the case of the attractive LJ potential: the first-order contribution,  $\xi_1(Q)$ , dominates if the tip does not come close enough to activate the LMs. If, however, it comes sufficiently close (that is, below  $Q_{crit}$  at the bottom of the oscillations), then the contribution of the LMs may become much stronger than that due to the first component in friction, especially for  $\tau \geq 400$ . In fact, one can find such values of  $\tau$  for which any desired dissipation energy is obtained. We stress, however, that in our model this will happen only in the case of the attractive tip–surface interaction when the tip comes sufficiently close to the surface during its oscillations.

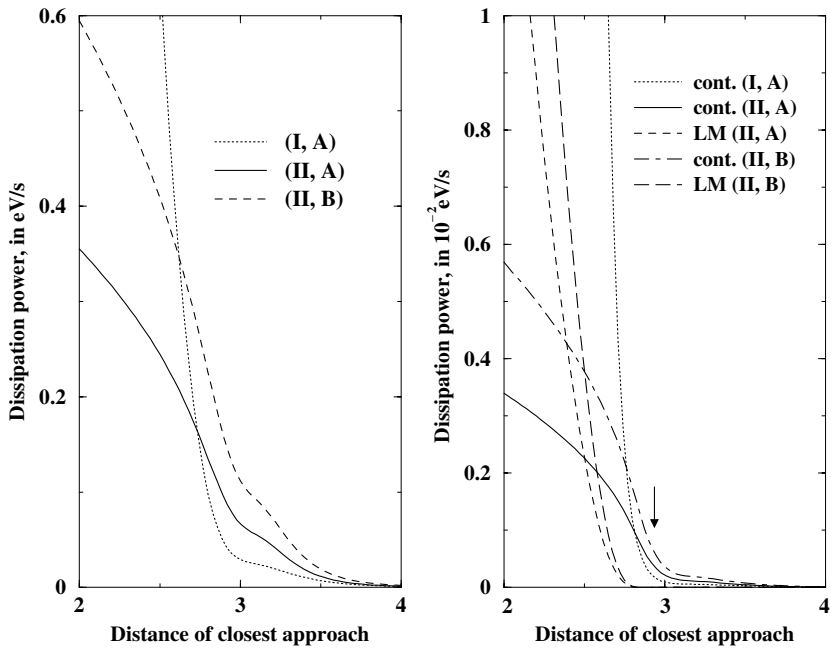


**Figure 4.** Dissipation power for the attractive LJ interaction potential versus the distance of the closest approach (in Å) for two oscillation amplitudes 36 Å (curves marked A) and 100 Å (marked B). The corresponding contributions due to the first-order,  $\xi_1(Q)$ , and second-order,  $\xi_2^{(1)}(Q)$  and  $\xi_2^{(2)}(Q)$ , terms are shown in the left and the right panels, respectively, for models I and II. The contributions from the surface phonon continuum ('cont.') and the LMs are given separately (for  $\tau = 10$ ). An arrow indicates the critical distance  $Q_{crit}$  for the LJ case.

## 5. Discussion

In this paper we re-examined our previous calculations [32] of the dissipation power for a model plane surface. Two new features have been introduced into the theory in order to verify the conclusion [30, 32] that the stochastic friction force mechanism produces dissipation energies which are deemed to be much smaller than those observed. We see that the new effects taken into account in this paper may lead to larger dissipation energies depending on whether the tip comes sufficiently close to the planar surface that local vibrational modes are induced. A critical distance at which the LMs split off from the phonon band depends on the actual character of the tip–surface interaction and, therefore, the lateral position of the tip with respect to the surface. We have also established a direct link between the dissipation effects and the strength of the coupling between the LMs and other surface phonons, i.e. anharmonicity. It follows from our calculations that for long-living LMs (weak coupling) the dissipation effects are actually larger. The reason for this is not clear and further studies are needed to shed light on this observation. It is also not clear at this stage whether the LMs can live long enough to ensure dissipation energies comparable with those observed in experiment. Molecular dynamics simulations may answer this question.

It is also likely that the dissipation effects are still underestimated in our simplified model and there are at least two reasons for that. First of all, the surface relaxation effects have not been properly treated here. In particular, in our model the surface dynamical matrix does not depend on the tip position  $Q$ . In practice, the equilibrium positions  $q_0(Q)$  of surface atoms

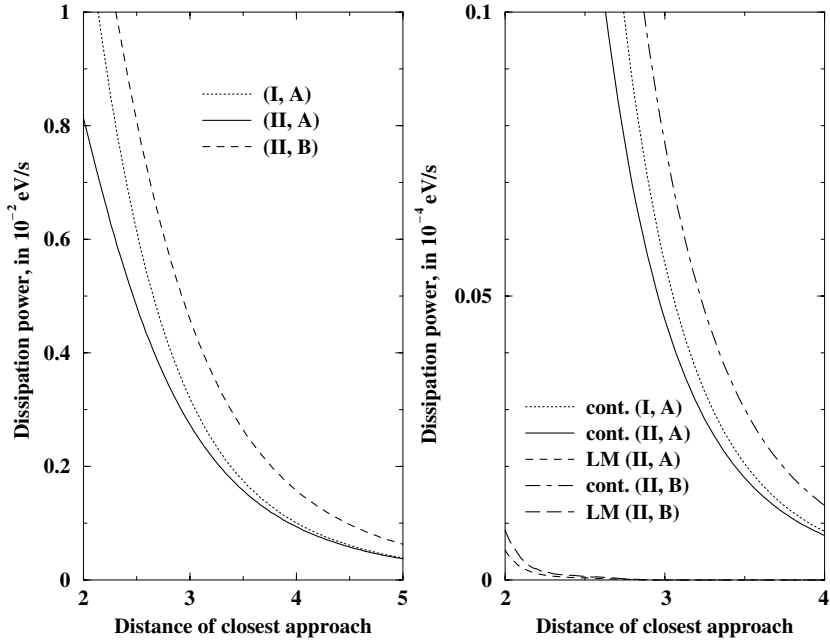


**Figure 5.** Dissipation power for the repulsive Coulomb interaction potential versus the distance of the closest approach. The notation is the same as in figure 4.

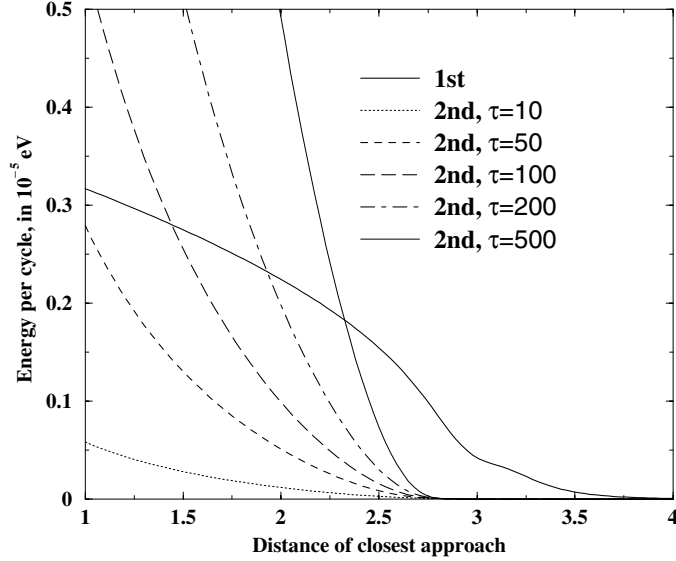


**Figure 6.** Dissipation energy per oscillation cycle (in eV) for the LJ potential as a function of the closest approach (in Å). Results for the first,  $\xi_1(Q)$ , and the second,  $\xi_2(Q) = \xi_2^{(1)}(Q) + \xi_2^{(2)}(Q)$ , contributions to the friction are shown separately for different values of  $\tau$ . The arrow indicates  $Q_{crit}$  and the oscillation amplitude  $A_0 = 36$  Å.

which change with the tip position  $Q$  would affect the dynamical matrix as well and, therefore, the Green function. If we assume that the tip comes sufficiently close to the surface during its

oscillations, substantial displacements (instabilities) of surface atoms may occur [34] resulting in significant change of the vibrations of surface atoms. If this effect is combined with the possibility that LMs can be induced at close approach, we may expect much larger dissipation energies. Secondly, for the tip-free system we have used essentially the bulk Green function. This means that possible *local surface modes* have been completely ignored in our approach. We may expect, however, that these states which are localized at the surface (but extended in the lateral directions) may interact strongly with the tip and result in additional enhancement of the dissipation energies. In this case LMs will exist at any  $Q$  and the corresponding contribution may start to be noticeable much earlier than the critical distance calculated here. Finally, one has to go beyond the simple model considered here and take into account interactions of *all* surface atoms with the tip; in addition, a more appropriate microscopic *model for the tip* is also needed. Therefore, more reliable models are necessary to address the points raised above. We are working in this direction at the moment.

It is well known [23, 30, 32] that the dissipation power is proportional to the square of the frequency. The dependence on the oscillation amplitude is not straightforward, however. We have checked this dependence and found that the dissipation effect increases with the growth of the amplitude in qualitative agreement with experiment [12].

We conclude this paper by saying that care is needed when comparing the calculated and measured dissipation energies. The dissipation energy is usually measured in terms of the amplitude of the driving (excitation) signal [12, 22]. However, as has been noted in [35], because of the non-linearity of the tip oscillations, the actual dissipation effects *due to energy transfer from the tip to the surface* could be much smaller. Note that we calculate precisely this part of the total energy loss, and there could be other losses in the system as well. Further investigation is necessary in this direction to completely clarify the issue.

## References

- [1] Fukui K, Onishi H and Iwasawa Y 1997 *Phys. Rev. Lett.* **79** 4202
- [2] Guggisberg M, Bammerlin M, Lüthi R, Loppacher Ch, Battiston F, Lü J, Baratoff A, Meyer E and Güntherodt H-J 1998 *Appl. Phys. A* **66** S245
- [3] Meyer E 1992 *Prog. Surf. Sci.* **41** 3
- [4] Giessibl F J 1995 *Science* **267** 68
- [5] Giessibl F J 1994 *Japan. J. Appl. Phys.* **33** 3726
- [6] Lüthi R, Meyer E, Bammerlin M, Baratoff A, Lehman T, Howard L, Gerber C and Güntherodt H-J 1996 *Z. Phys. B* **100** 165
- [7] Güntherodt H-J, Anselmetti D and Meyer E (ed) 1995 *Forces in Scanning Probe Methods (NATO Advanced Study Institute Series E: Applied Sciences, vol 286)* (Dordrecht: Kluwer)
- [8] Sugawara Y, Ohta M, Ueyama H, Morita S, Osaka F, Ochkouchi S, Suzuki M and Mishima S 1996 *J. Vac. Sci. Technol.* **14** 953
- [9] Erlandsson R, Olsson L and Mårtensson P 1996 *Phys. Rev. B* **54** R8309
- [10] Bammerlin M, Lüthi R, Meyer E, Baratoff A, Guggisberg M, Gerber C, Howard L and Güntherodt H-J 1997 *Probe Microsc.* **1** 3
- [11] Bennewitz R, Foster A S, Kantorovich L N, Bammerlin M, Loppacher Ch, Schar S, Guggisberg M, Meyer E and Shluger A L 2000 *Phys. Rev. B* **62** 2074
- [12] Loppacher C, Bennewitz R, Pfeiffer O, Guggisberg M, Bammerlin M, Schär S, Barwich V, Baratoff A and Meyer E 2000 *Phys. Rev. B* **62** 13 674
- [13] Lantz M A, Hug H J, van Schendel P J A, Hoffmann R, Martin S, Baratoff A, Abdurixit A, Güntherodt H-J and Gerber Ch 2000 *Phys. Rev. Lett.* **84** 2642
- [14] Dürig U 1999 *Surf. Interface Anal.* **27** 467
- [15] Gotsmann B and Fuchs H 2001 *Phys. Rev. Lett.* **86** 2597
- [16] Shluger A L, Livshits A I, Foster A S and Catlow C R A 1999 *J. Phys.: Condens. Matter* **11** R295
- [17] Livshits A I, Shluger A L, Rohl A L and Foster A S 1999 *Phys. Rev. B* **59** 2436
- [18] Giessibl F J 1997 *Phys. Rev. B* **56** 16 010

- [19] Sasaki N and Tsukada M 1999 *Appl. Surf. Sci.* **140** 339
- [20] Abdurxit A, Baratoff A and Meyer E 2000 *Appl. Surf. Sci.* **157** 355
- [21] Cleveland J P, Anczykowski B, Schmid A E and Elings V B 1998 *Appl. Phys. Lett.* **72** 2613
- [22] Anczykowski B, Gotsmann B, Fuchs H, Cleveland J P and Elings V B 1999 *Appl. Surf. Sci.* **140** 376
- [23] Gotsmann B, Seidel C, Anczykowski B and Fuchs H 1999 *Phys. Rev. B* **60** 11051
- [24] Molitor S, Güther P and Berghausen T 1999 *Appl. Surf. Sci.* **140** 276
- [25] Sasaki N and Tsukada M 2000 *Japan. J. Appl. Phys.* **39** L1334
- [26] García R, Tamayo J and San Paulo A 1999 *Surf. Interface Anal.* **27** 312
- [27] Kantorovich L 2001 *J. Phys.: Condens. Matter* **13** 945
- [28] Dorofeyev I, Fuchs H, Wenning G and Gotsmann B 1999 *Phys. Rev. Lett.* **83** 2402
- [29] Persson B N J and Volokitin A I 2000 *Phys. Rev. Lett.* **84** 3504
- [30] Gauthier M and Tsukada M 1999 *Phys. Rev. B* **60** 11716
- [31] Mo Man Yue and Kantorovich L 2001 *J. Phys.: Condens. Matter* **13** 1439
- [32] Kantorovich L N 2001 *Phys. Rev. B* **64** 245409
- [33] Layzer A *J. Phys. Rev.* 1963 **129** 897
- [34] Shluger A L, Kantorovich L N, Livshits A I and Gillan M J 1997 *Phys. Rev. B* **56** 15332
- [35] Gauthier M and Tsukada M 2000 *Phys. Rev. Lett.* **85** 5348